

AD-A129 473

ASYMPTOTIC INVISCID THEORY OF LIFT ON SLENDER BODIES OF 1/1
REVOLUTION(U) AERONAUTICAL RESEARCH ASSOCIATES OF
PRINCETON INC NJ J E YATES FEB 83 ARAP-493

UNCLASSIFIED

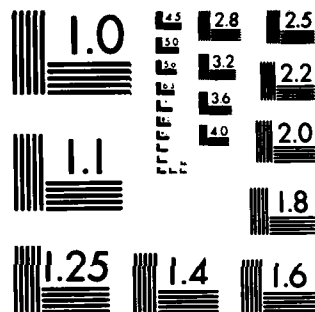
N00014-82-C-0352

F/G 20/4

NL

END
DATE
FILMED

7 83
DTIC



MICROCOPY RESOLUTION TEST CHART
NATIONAL BUREAU OF STANDARDS-1963-A

ADA129473

UNCLASSIFIED

SECURITY CLASSIFICATION OF THIS PAGE (When Data Entered)

REPORT DOCUMENTATION PAGE		READ INSTRUCTIONS BEFORE COMPLETING FORM
1. REPORT NUMBER	2. GOVT ACCESSION NO. AD A129473	3. RECIPIENT'S CATALOG NUMBER
4. TITLE (and Subtitle) ASYMPTOTIC INVISCID THEORY OF LIFT ON SLENDER BODIES OF REVOLUTION		5. TYPE OF REPORT & PERIOD COVERED Final 4/15/82 - 1/14/83
7. AUTHOR(s) John E. Yates		6. PERFORMING ORG. REPORT NUMBER A.R.A.P. Report No. 493
9. PERFORMING ORGANIZATION NAME AND ADDRESS Aeronautical Research Associates of Princeton, Inc. 50 Washington Road, P. O. Box 2229 Princeton, New Jersey 08540		8. CONTRACT OR GRANT NUMBER(s) N00014-82-C-0352
11. CONTROLLING OFFICE NAME AND ADDRESS Office of Naval Research, Dept. of the Navy 800 N. Quincy Street Arlington, Virginia 22217		10. PROGRAM ELEMENT, PROJECT, TASK AREA & WORK UNIT NUMBERS 61153N RR023-01-01 NR 062-733
14. MONITORING AGENCY NAME & ADDRESS (if different from Controlling Office)		12. REPORT DATE February 1983
		13. NUMBER OF PAGES 28
		15. SECURITY CLASS. (of this report) Unclassified
		15a. DECLASSIFICATION/DOWNGRADING SCHEDULE
16. DISTRIBUTION STATEMENT (of this Report) Approved for public release, distribution unlimited.		
17. DISTRIBUTION STATEMENT (of the abstract entered in Block 20, if different from Report)		
18. SUPPLEMENTARY NOTES		
19. KEY WORDS (Continue on reverse side if necessary and identify by block number) Incompressible Lift Slender Bodies Eigenfunction		
20. ABSTRACT (Continue on reverse side if necessary and identify by block number) The viscous theory of lift on bodies of revolution developed under previous contract (ONR N00014-81-C-0240) is simplified for slender bodies of revolution. The resultant inviscid integral equation is solved in closed form for a prolate spheroidal body. An explicit representation of the eigenfunction is obtained and numerical results for the load distribution are compared with results of conventional slender body theory. The magnitude of the eigenfunction is estimated to be of order 1 by correlating with experimental data on the		

DD FORM 1 JAN 73 1473

EDITION OF 1 NOV 65 IS OBSOLETE

UNCLASSIFIED

SECURITY CLASSIFICATION OF THIS PAGE (When Data Entered)

UNCLASSIFIED

SECURITY CLASSIFICATION OF THIS PAGE(When Data Entered)

USS Akron. The qualitative features of the load distribution are in much better agreement with experimental data than the distribution obtained with the equivalent base area concept applied to conventional slender body theory.

UNCLASSIFIED

SECURITY CLASSIFICATION OF THIS PAGE(When Data Entered)

TABLE OF CONTENTS

NOMENCLATURE	iii
I. INTRODUCTION	1
II. ASYMPTOTIC STEADY STATE THEORY	3
III. SOLUTION OF THE FUNDAMENTAL INTEGRAL EQUATION FOR A PROLATE SPHEROIDAL BODY	13
IV. CONCLUSIONS	25
V. REFERENCES	27



Accession For	
NTIS GRA&I	<input checked="" type="checkbox"/>
DTIC TAB	<input checked="" type="checkbox"/>
Unannounced	<input type="checkbox"/>
Justification	<input type="checkbox"/>
Distribution/	
Availability Codes	
Dist	Avail and/or Special
A	

NOMENCLATURE

A_n	coefficients that define the load function, see Eqs. (3.2) and (3.7)
A'_0	see Eq. (3.26)
B_z	incomplete Beta function
C_M	moment coefficient, see Eq. (2.11)
C_N	normal force coefficient, see Eq. (2.11)
\bar{C}_M	see Eq. (3.31)
\bar{C}_N	see Eq. (3.31)
$c_N(x)$	normal force coefficient per unit length, see Eq. (3.20)
$E(k)$	elliptic integral of second kind (see Eq. (2.4))
$F(x)$	inviscid eigenfunction, see Eqs. (3.8) and (3.9)
$\mathcal{F}(z)$	hypergeometric function, see Eqs. (3.12) and (3.16)
$f(x)$	see Eq. (2.20)
$\mathcal{G}(x, r, \rho)$	see Eq. (2.3)
g_0^N	see Eqs. (3.27) and (3.28)
$g(x)$	see Eq. (3.25) and Fig. 3.1
$H(x)$	heaviside step function
$\mathcal{H}(x, \xi)$	kernel function (see Eq. (2.2))
$\mathcal{H}_0(x, \xi)$	conventional slender body kernel function, see Eq. (2.24)
$K(k)$	elliptic integral of first kind (see Eq. (2.5))
k	see Eq. (2.6)
L	total lift, see Eq. (2.10a)

PROCEEDING PAGE BLANK-NOT FILMED

$L(x)$	normalized load function
$\mathcal{L}(x)$	load function (see Eq. 2.9))
l	$x_T - x_N$, body length
$l(x)$	normal force per unit length
M	total moment about center of body, see Eq. (2.10b)
q_o	$ \vec{v}_o $ surface speed
R_o	reference body radius
$R(x)$	body radius, see Fig. 2.1
$R'(x)$	dR/dx , body slope
S	$= \pi R^2$, body cross-sectional area
$T_n(x)$	Chebyshev polynomial of the first kind
$U_n(x)$	Chebyshev polynomial of the second kind
V	body volume
\vec{v}_o	axial flow surface velocity
v_∞	free stream velocity
$\mathcal{W}_g(x)$	upwash function (see Eq. (2.8))
x_N, x_T	axial locations of the nose and tail of the body of revolution
x_o	see Eqs. (3.28) and (3.29)
x, r, θ	cylindrical coordinate (see Fig. 2.1)
α	angle of attack
ϵ	$2R_o/l$
ρ_∞	free stream density

$\tau(x)$ $2R(x)/l$, normalized body radius

τ_0 $2R_0/l$

I. INTRODUCTION

The viscous theory of lift on bodies of revolution is developed in detail in Ref. 1. The problem of calculating lift on a body is reduced to one of solving an integral equation of the first kind, in complete analogy with the theory of lift on wing sections. Whereas the theory is formally well developed, specific results are difficult to obtain due to the complexity of the associated kernel function. In Ref. 1, an explicit evaluation of the kernel function was carried out and load calculations were made for the case of a ring-wing, a degenerate but highly useful form of a body of revolution. The results obtained were in agreement with a theoretical result of Ribner (Ref. 2) and with experimental data of Flatau (Ref. 3).

In the present report, the theory is simplified by deriving the asymptotic form of the kernel function for slender bodies of revolution. The resulting inviscid integral equation is solved in closed form for the case of a prolate spheroidal body. An explicit representation of the inviscid eigenfunction is obtained and numerical results for the lift distribution are compared with results of conventional slender body theory. Also, the magnitude of the eigenfunction is estimated by correlating with experimental data on the USS Akron. The qualitative features of the load distribution are in much better agreement with experimental data than the distribution obtained with the equivalent base area concept applied to conventional slender body theory.

PRECEDING PAGE BLANK-NOT FILMED

II. ASYMPTOTIC STEADY STATE THEORY

The point of departure for the present study is the inviscid integral Eq. (2.35) of Ref. 1; i.e.,

$$\frac{1}{2\pi} \int_{x_N}^{x_T} L(\xi) \mathcal{K}(x, \xi) d\xi = W_g(x)/v_\infty \quad (2.1)$$

where $L(x)$ is the unknown load function, $W_g(x)$ is a specified upwash function and $\mathcal{K}(x, \xi)$ is the kernel function. The definition of the steady state kernel function is

$$\mathcal{K}(x, \xi) = \lim_{r \rightarrow R(x)} \int_{\xi}^{\infty} \left(\frac{\partial^2 \mathcal{G}}{\partial N \partial N'} \right)_{\rho=R(\xi')} R(\xi') d\xi' \quad (2.2)$$

where

$$\begin{aligned} \mathcal{G}(x, r, \rho) &= \int_0^{2\pi} \frac{\cos \theta d\theta}{\sqrt{x^2 + r^2 + \rho^2 - 2rp \cos \theta}} \\ &= -\frac{4}{\sqrt{x^2 + (r+\rho)^2}} \left[\left(1 - \frac{2}{k^2}\right) K(k) + \frac{2}{k^2} E(k) \right] \end{aligned} \quad (2.3)$$

with the standard elliptic integrals (see Ref. 4, p. 589)

$$E(k) = \int_0^{\pi/2} \sqrt{1 - k^2 \sin^2 \theta} d\theta \quad (2.4)$$

$$K(k) = \int_0^{\pi/2} \frac{d\theta}{\sqrt{1 - k^2 \sin^2 \theta}} \quad (2.5)$$

where

PROCEEDING PAGE BLANK-NOT FILLED

$$k^2 = \frac{4rp}{x^2 + (r+p)^2} \quad (2.6)$$

Also

$$\frac{\partial}{\partial N} = -R'(x) \frac{\partial}{\partial x} + \frac{\partial}{\partial r}, \quad \frac{\partial}{\partial N'} = -R'(\xi') \frac{\partial}{\partial \xi'} + \frac{\partial}{\partial \rho} \quad (2.7)$$

and $R(x)$ is the specified body and wake control surface shape (see Figure 2.1).

For the remainder of this report we consider a body of revolution at constant angle of attack α . To lowest order in body thickness the upwash function becomes

$$\frac{W_g(x)}{v_\infty} = - \frac{i \cdot v_o}{v_\infty} \cdot \alpha = - \frac{(q_o/v_\infty)}{\sqrt{1 + R'^2}} \alpha \quad (2.8a)$$

$$\approx -\alpha \quad \text{for slender bodies} \quad (2.8b)$$

The approximation made in Eq. (2.8b) is not valid near the fore and aft ends of the body where the flow stagnates. In these regions one should use Eq. (2.8a) with the calculated or measured axial flow surface speed, q_o .

The unknown load function $\mathcal{L}(x)$ in Eq. (2.1) is related to the normal force per unit length on the body $l(x)$ via the following relation:

$$l(x) = \frac{1}{2} \rho_\infty v_\infty^2 \cdot \left(\frac{q_o}{v_\infty} \right) \cdot (2\pi R(x)) \cdot \mathcal{L}(x) \quad (2.9)$$

The total lift and moment about the y axis are given respectively by

$$L = \int_{x_N}^{x_T} l(x) dx \quad (2.10a)$$

and

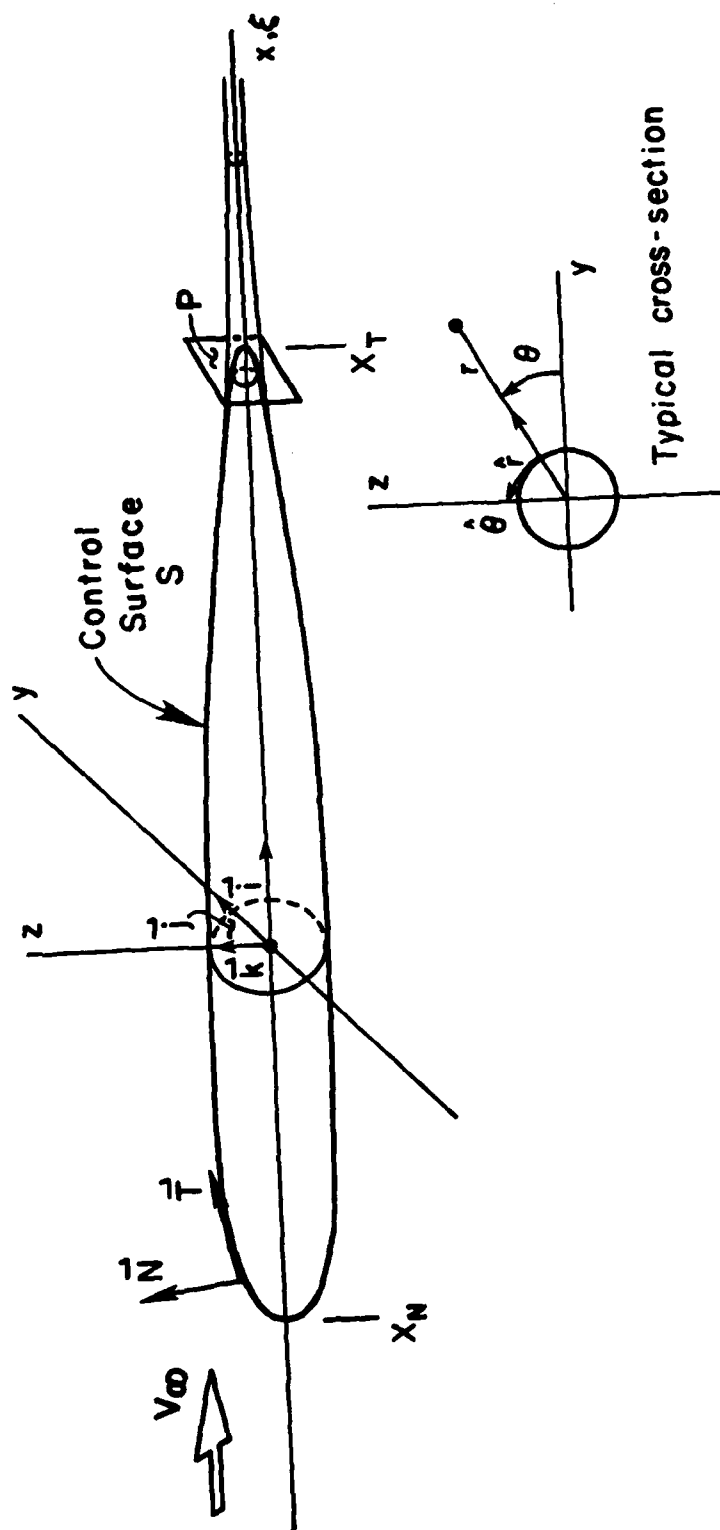


Figure 2.1 Body of Revolution and Enveloping Control Surface.

$$M = - \int_{x_N}^{x_T} x \cdot l(x) dx \quad (2.10b)$$

Let $l = (x_T - x_N)$ denote the total body length and define the normal force and moment coefficients as follows:

$$C_N = \frac{L}{1/2 \rho_\infty v_\infty^2 \pi R_0 \cdot l} \quad \text{Normal Force Coefficient}$$

$$C_M = \frac{M}{1/2 \rho_\infty v_\infty^2 \pi R_0 \cdot l \cdot (l/2)} \quad \text{Moment Coefficient} \quad (2.11)$$

where R_0 is a reference body radius; e.g. the radius at the maximum girth or center of buoyancy. Substitute Eq. (2.9) into the formulas (2.11) to obtain

$$C_N = \int_{-1}^1 \mathcal{L}(x) \cdot \left(\frac{q_0}{v_\infty} \right) \cdot \frac{R(x)}{R_0} \cdot dx$$

and

$$C_M = - \int_{-1}^1 \mathcal{L}(x) \cdot x \cdot \left(\frac{q_0}{v_\infty} \right) \cdot \frac{R(x)}{R_0} \cdot dx \quad (2.12)$$

In the last two formulas and in the remainder of this report we choose the body half length ($l/2$) as a reference length and further choose the origin of coordinates at the body mid-length. All integrals over the body then become integrals from -1 to 1 in normalized coordinates. The moment is about the center of the body and is positive nose up.

The most important step in reducing the integral Eq. (2.1) to a more tractable form is to introduce the slender body approximation; i.e.,

$$R(x) \ll l/2 \quad (2.13)$$

The kernel function (see Eq. (2.2)) can then be approximated by a relatively simple expression. For load points, ξ , that are far removed from the upwash control point, x ; i.e.,

$$|x-\xi| \gg R(x) \quad (2.14)$$

the kernel function can be replaced by the classical slender body kernel as we demonstrate below. For load points close to the upwash control point; i.e.,

$$|x-\xi| \ll R(x) \quad (2.15)$$

the kernel can be replaced by a local ring-wing approximation. We turn now to a detailed derivation of these results.

For the case covered by Eq. (2.14), we recognize that the parameter k in Eq. (2.3) is much less than unity so that

$$\mathcal{G}(k, r, \rho) = \frac{\pi r \rho}{x^3} \left(1 + O(k^2) \right), \quad k \ll 1 \quad (2.16)$$

and

$$R(\xi') \frac{\partial^2 \mathcal{G}}{\partial N \partial N'} = \frac{\pi R(\xi')}{|x-\xi'|^3} \quad (2.17)$$

Thus, for

$$x \ll \xi$$

we have

$$\begin{aligned} \mathcal{K}(x, \xi) &= \int_{\xi}^{\infty} \frac{\pi R(\xi')}{(\xi' - x)^3} d\xi' \\ &= \frac{\pi R(\xi)}{2(\xi - x)^2} \end{aligned} \quad (2.18)$$

For

$$x \gg \xi$$

we write Eq. (2.2) in the following form:

$$\begin{aligned} \mathcal{H}(x, \xi) &= \lim_{r \rightarrow R(x)} \int_{-\infty}^{\infty} \frac{\partial^2 \mathcal{G}}{\partial N \partial N'} R(\xi') d\xi' - \int_{-\infty}^{\xi} \left(\frac{\partial^2 \mathcal{G}}{\partial N \partial N'} \right)_{r=R(x)} R(\xi') d\xi' \\ &\approx f(x) - \frac{\pi R(\xi)}{2(x-\xi)^2} \end{aligned} \quad (2.19)$$

where the second term is obtained with the same approximation that led to Eq. (2.18). The function $f(x)$ can be inferred from our ring-wing results as follows. Note that

$$f(x) = \lim_{r \rightarrow R(x)} \int_{-\infty}^{\infty} \frac{\partial^2 \mathcal{G}}{\partial N \partial N'} R(\xi') d\xi' \quad (2.20)$$

and furthermore, that the principal contribution to the integrand is for points ξ' near x . Thus, we replace $R(\xi')$ by $R(x)$ and let

$$\frac{\partial^2}{\partial N \partial N'} = \frac{\partial^2}{\partial r \partial \rho} \quad (2.21)$$

in Eq. (2.20). The result is

$$f(x) = \lim_{r, \rho \rightarrow R(x)} R(x) \int_{-\infty}^{\infty} \frac{\partial^2 \mathcal{G}}{\partial r \partial \rho} d\xi' \quad (2.22)$$

$$\approx - \frac{2\pi}{R(x)} \quad (2.23)$$

where we have noted that Eq. (2.22) is the asymptotic form of the ring-wing kernel (see Eqs. (2.42) and (2.45) of Ref. 1).

With Eqs. (2.18) and (2.19) we can express the kernel function of classical slender body theory in the form

$$\mathcal{K}_0(x, \xi) = -\frac{2\pi}{R(x)} \left[H(x-\xi) + O\left(\frac{R^2(x)}{|x-\xi|^2}\right) \right] \quad (2.24)$$

If we neglect the second term, the integral equation of slender body theory becomes (here we use dimensional coordinates)

$$\frac{1}{2\pi} \int_{x_N}^x \mathcal{L}(\xi) \left(-\frac{2\pi}{R(x)} \right) d\xi = \frac{W_g(x)}{v_\infty}$$

or

$$\int_{x_N}^x \mathcal{L}(\xi) d\xi = \frac{R(x)(q_0/v_\infty)}{\sqrt{1+R'^2}} \cdot \alpha \quad (2.25)$$

so that

$$\mathcal{L}(x) = \frac{d}{dx} \left\{ \frac{R(x)(q_0/v_\infty)}{\sqrt{1+R'^2}} \right\} \alpha \quad (2.26)$$

Substitute the last result into Eq. (2.9) to obtain the lift per unit length.

$$l_0(x) = \rho_\infty v_\infty^2 \cdot \pi \cdot R(x)(q_0/v_\infty) \cdot \frac{d}{dx} \left\{ \frac{R(x)(q_0/v_\infty)}{\sqrt{1+R'^2}} \right\} \alpha \quad (2.27)$$

If all second order effects of slope are neglected, then we obtain the classical slender body formula.

$$l_0(x) = \frac{\rho_\infty v_\infty^2}{2} \frac{dS}{dx} \cdot \alpha \quad (2.28)$$

with

$$S = \pi R^2(x) \quad (2.29)$$

A slight modification of Eq. (2.28) that forces the lift per unit length to zero at blunt ends is obtained by replacing the body radius $R(x)$ by $R(x)(q_0/v_\infty)$. This is tantamount to neglecting the factor $\sqrt{1 + R'^2}$ in the denominator of Eq. (2.27). Alternatively, we can replace the dynamic pressure in Eq. (2.28) by its local value $(\rho_\infty q_0^2/2)$. Since we do not rigorously calculate second order corrections for body slope, all of the foregoing approximations are formally equivalent.

We pointed out in Ref. 1 (p. 17) that the most significant nonuniformity of classical slender body theory is due to the ad hoc elimination of the Cauchy singularity in the fundamental integral Eq. (2.1). (See Figure 2.2 for a comparison of singularities in the various kernels.) The main theoretical result of this study is the correction of the classical slender body kernel (Eq. (2.24)) that retains the essential Cauchy singularity. This step permits us to calculate the inviscid eigenfunction and to introduce the effect of viscosity to determine the magnitude of the eigenfunction.

To obtain the correct lowest order slender body kernel function we evaluate Eq. (2.2) for $|x-\xi| \ll R(x)$. We have already seen from our ring-wing calculation that $\mathcal{K}(x, \xi)$ is singular. Furthermore, we can use the ring-wing result directly since to lowest order in thickness, a slender body can be approximated locally by a cylindrical surface. Thus, from Eqs. (2.41) and (2.46) of Ref. 1,

$$\mathcal{K}(x, \xi) = -\frac{2}{x-\xi} \quad \text{for } |x-\xi| \ll R(x) \quad (2.30)$$

The complete asymptotic kernel function is obtained by adding Eq. (2.30) and the principal part of Eq. (2.24). Thus

$$\mathcal{K}(x, \xi) = -\frac{2}{x-\xi} - \frac{2\pi}{R(x)} H(x-\xi) \quad (2.31)$$

Substitute Eq. (2.31) into Eq. (2.1) and multiply the resulting equation by

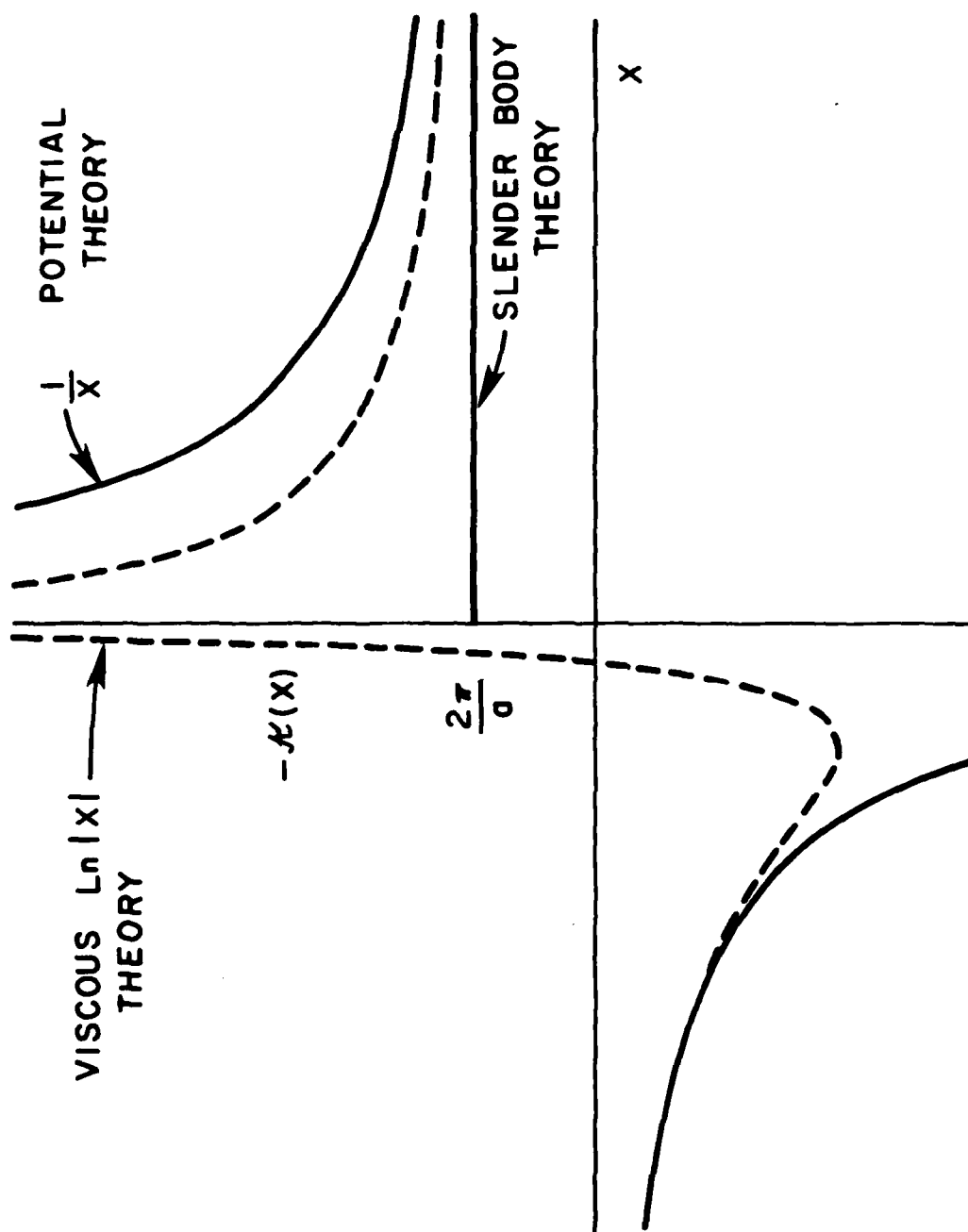


Figure 2.2 Comparison of the Inviscid and Viscous Kernels and the Slender Body Kernel for a Ring-Wing (Ref. 1).

(-R(x)) to get (in normalized coordinates)

$$\frac{\tau(x)}{\pi} \int_{-1}^1 \frac{L(y)}{x-y} dy + \int_{-1}^x L(y) dy = \tau(x) \alpha(x) \quad (2.32)$$

where

$$\alpha(x) = \frac{q_0/v_\infty}{\sqrt{1 + R'^2}} \cdot \alpha \approx \alpha \quad (2.33)$$

$$\tau(x) = \frac{2R(x)}{l} \quad (2.34)$$

and $L(x)$ is the load function $\mathcal{L}(x)$ expressed in terms of the dimensionless axial coordinate.

The slender body integral Equation (2.32) is the fundamental theoretical result of this report. We investigate the solution of this equation in the following section. In conclusion, we remark that for $\tau(x) \ll 1$, and with the classical slender body approximation, we recover the result of Equation (2.25). On the other hand, for $\tau(x) \gg 1$, we obtain

$$\frac{1}{\pi} \int_{-1}^1 \frac{L(y)}{x-y} dy = \alpha(x) \quad (2.35)$$

the integral equation of wing theory or actually the limiting case of ring-wing theory with an infinite diameter to length ratio. It is essential that both terms be retained in Eq. (2.32) to obtain correct slender body results.

III. SOLUTION OF THE FUNDAMENTAL INTEGRAL EQUATION FOR A PROLATE SPHEROIDAL BODY

Consider the body shape

$$\tau(x) = \epsilon \sqrt{1 - x^2}, \quad |x| < 1, \quad \epsilon \ll 1 \quad (3.1)$$

and suppose that the wake control surface (see Figure 2.1) has been collapsed onto the line extending downstream to infinity from the aft most position on the body. Next, we assume a load function of the form

$$L(x) = \frac{1}{\sqrt{1 - x^2}} \sum_{n=0}^{\infty} A_n T_n(x) \quad (3.2)$$

where

$$T_n(\cos\theta) = \cos n\theta, \quad x = \cos\theta \quad (3.3)$$

The last expression defines the Chebyshev polynomials of the first kind, $T_n(x)$ (Ref. 4, p. 776). Now substitute Eqs. (3.1) and (3.2) into Eq. (2.32). The result is

$$A_0 \left(\frac{\pi}{2} + \sin^{-1} x \right) - \sqrt{1 - x^2} \sum_{n=1}^{\infty} A_n \left(\epsilon + \frac{1}{n} \right) U_{n-1}(x) = \epsilon \alpha \sqrt{1 - x^2} \quad (3.4)$$

where

$$U_n(\cos\theta) = \frac{\sin(n+1)\theta}{\sin\theta} \quad (3.5)$$

The last expression defines the Chebyshev polynomials of the second kind, $U_n(x)$. Finally, multiple Eq. (3.4) by $U_m(x)$ and integrate over x to obtain the following:

$$2A_0 - (1 + \epsilon)A_1 = \epsilon \alpha \quad n=1 \quad (3.6a)$$

$$2A_0 - (1 + \epsilon n)A_n = 0 \quad n=2,3,\dots \quad (3.6b)$$

Thus, we obtain for the coefficients A_n that define the load function,

$$A_1 = \frac{2}{1 + \epsilon} A_0 - \frac{\epsilon \alpha}{1 + \epsilon} \quad (3.6)$$

$$A_n = \frac{2}{1 + \epsilon n} A_0 \quad n=2,3,\dots \quad (3.7)$$

The coefficient A_0 is completely arbitrary.

With the foregoing results we can express the load function as follows:

$$L(x) = -\frac{\epsilon \alpha}{1 + \epsilon} \cdot \frac{x}{\sqrt{1 - x^2}} + A_0 \frac{F(x)}{\sqrt{1 - x^2}} \quad (3.8)$$

where

$$F(x) = 2f(x) - 1 \quad (3.9)$$

and

$$f(x) = \sum_{n=0}^{\infty} \frac{T_n(x)}{1 + n\epsilon} \quad (3.10)$$

The first term in Eq. (3.8) is the particular solution of Eq. (2.32) and is essentially the same result that one would obtain with classical slender body theory. The second term is the important new result. It is the eigenfunction multiplied by the arbitrary coefficient A_0 . We now derive an explicit functional relation for the eigenfunction $F(x)$.

Use the definition (3.3) in Eq. (3.11) to obtain

$$g(\theta) = f(\cos \theta) = \operatorname{Re} \mathcal{F}(e^{i\theta}) \quad (3.11)$$

where

$$\mathcal{F}(z) = \sum_{n=0}^{\infty} \frac{z^n}{1 + n\epsilon} \quad (3.12)$$

Now it can readily be shown that $\mathcal{F}(z)$ satisfies the first order differential equation

$$\epsilon z \mathcal{F}'(z) + \mathcal{F}(z) = \frac{1}{1 - z} \quad (3.13)$$

with the boundary condition

$$\mathcal{F}(0) = 1 \quad (3.14)$$

Thus, we integrate Eq. (3.14) to obtain

$$\begin{aligned} \mathcal{F}(z) &= \frac{z^{-1/\epsilon}}{\epsilon} \int_0^z \frac{\zeta^{1/\epsilon-1}}{1 - \zeta} d\zeta \\ &= \frac{1}{\epsilon} \int_0^1 \frac{t^{1/\epsilon-1}}{1 - zt} dt \end{aligned} \quad (3.15)$$

From Ref. 4, p. 558, we find that $F(z)$ can be expressed in terms of the standard hypergeometric function; i.e.,

$$\mathcal{F}(z) = F(1, 1/\epsilon; 1 + 1/\epsilon, z) \quad (3.16)$$

or the incomplete Beta function (see Ref. 4, p. 263)

$$\mathcal{F}(z) = \frac{z^{1/\epsilon}}{\epsilon} B_z(1/\epsilon, 0) \quad (3.17)$$

With either Eq. (3.16) or (3.17) the eigenfunction is completely defined for

arbitrary fineness ratio ($1/\epsilon$). For the special case that ϵ is the reciprocal of an integer; i.e.,

$$\epsilon = 1/N \quad (3.18)$$

where N is the body fineness ratio, we can express $f(x)$ in terms of elementary functions. The result is

$$f(\cos\theta) = -N \left[\frac{(\theta - \pi)}{2} \sin N\theta + \cos N\theta \cdot \ln(2 \sin\theta/2) + \sum_{n=1}^{N-1} \frac{\cos n\theta}{(N-n)} \right] \quad (3.19)$$

Note that $f(\cos\theta)$ has a logarithmic singularity at $\theta = 0$; i.e., at the body aft end. Also, we remark that even though the eigenfunction is expressed as a finite sum of oscillatory trigonometric functions, the actual eigenfunction is a smooth function of x as we show below.

To complete the inviscid theoretical work in this report, we derive expressions for the load distribution and the total normal force and moment coefficients. Define the normal force coefficient per unit normalized length as

$$\begin{aligned} c_N(x) &= L(x) \cdot \frac{q_o}{v_\infty} \cdot \frac{R(x)}{R_o} \\ &= L(x) \cdot \frac{q_o}{v_\infty} \cdot \frac{\tau(x)}{\tau_o} \end{aligned} \quad (3.20)$$

where

$$\tau_o = \frac{2R_o}{l} \quad (3.21)$$

Then from Eqs. (2.12), we have

$$C_N = \int_{-1}^1 c_N(x) dx$$

$$C_M = - \int_{-1}^1 c_N(x) \cdot x dx \quad (3.22)$$

Substitute Eqs. (3.1) and (3.8) into Eq. (3.20) and let $\tau_0 = \epsilon$ to obtain

$$c_N(x) = - \frac{\epsilon \alpha}{(1 + \epsilon)} \cdot \left(\frac{q_0 x}{v_\infty} \right) + A_0 \cdot \left(\frac{q_0}{v_\infty} F(x) \right) \quad (3.23)$$

Since $q_0(x)$ is a symmetric function of x for a symmetrical body, we further obtain

$$C_N = A_0 \int_{-1}^1 \frac{q_0}{v_\infty} F(x) dx$$

and

$$C_M = + \frac{\epsilon \alpha}{1 + \epsilon} \int_{-1}^1 \frac{q_0 x^2}{v_\infty} dx - A_0 \int_{-1}^1 \frac{q_0}{v_\infty} x \cdot F(x) dx \quad (3.24)$$

An important conclusion can be made at once from the foregoing results. The normal force coefficient is proportional to the magnitude of the eigenfunction in complete analogy with the theoretical lift coefficient on a wing section. Furthermore, this conclusion is not limited to a prolate spheroidal body. The general form of $c_N(x)$ is the slender body distribution of load plus the contribution of the eigenfunction. For a closed body the first part always integrates to zero. With the present formulation it is not necessary to introduce an artificial base area. Experimental normal force data can be correlated in terms of A_0 and the complete normal force distribution can be calculated with Eq. (3.23).

Examples of the theoretical normal force distribution are presented in Figure 3.1. We actually plot the approximate load function

$$g(x) = \left(\frac{1 + \epsilon}{\alpha \epsilon} \right) \left(\frac{v_\infty}{q_0} \right) \cdot c_N(x)$$

$$= -x + A'_0 F(x) \quad (3.25)$$

where

$$A'_0 = \left(\frac{1 + \epsilon}{\epsilon \alpha} \right) \cdot A_0 = \frac{1 + \epsilon}{\epsilon} \left(\frac{dA_0}{d\alpha} \right)_{\alpha=0} \quad (3.26)$$

As a brief aside, the surface speed q_0 on a prolate spheroidal body is known in closed form (see Ref. 5, p. 141, Eq. 4 for the potential function) and is proportional to $(1/\sqrt{1 + R'^2})$. We omit all blunt end mean flow effects in the following comparison in order to stress the differences between conventional slender body theory and the present theory that includes the eigenfunction. The end effects must definitely be included as the theory is refined into a working tool.

For $A'_0 = 0$, we obtain the conventional slender body result (so labeled in Figure 3.1). The eigenfunction $F(x)$ is plotted for body fineness ratios, $N = 7$ and 11. Recall that the eigenfunction can be evaluated with Eq. (3.19) when ϵ is the reciprocal of an integer. The eigenfunction for $N = 7$ is added to the slender body load to obtain the curves for $A'_0 = 1/2$ and 1. It is an interesting and physically appealing feature of the theory that the slender body load distribution is very good over the forward portion of the body. The nature of the eigenfunction is such that the negative slender body load on the aft section of the body is reduced. In Figure 3.2 (taken from Ref. 6) the theoretical and measured load distribution on the USS Akron are compared. Even though the results presented are well into the nonlinear angle of attack region ($\alpha = 12$ deg), it is noted that slender body or Munk theory is not too bad over the forward 65% of the hull. The deviation between slender body theory and experiment also has the same qualitative features as the differences indicated in our theoretical Figure 3.1.

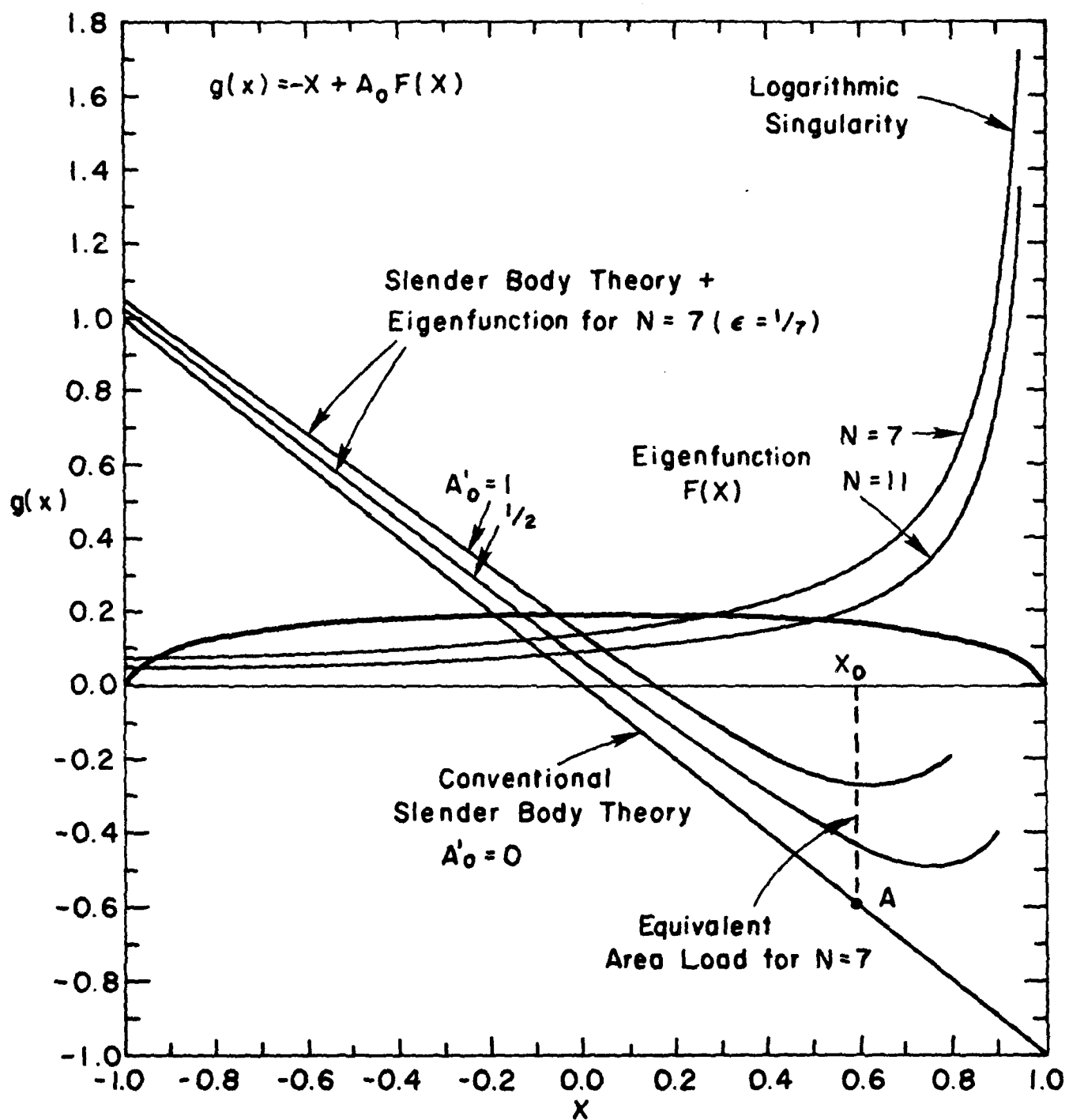


Figure 3.1 Load Distribution on a Prolate Ellipsoid of Revolution at Constant Angle of Attack.

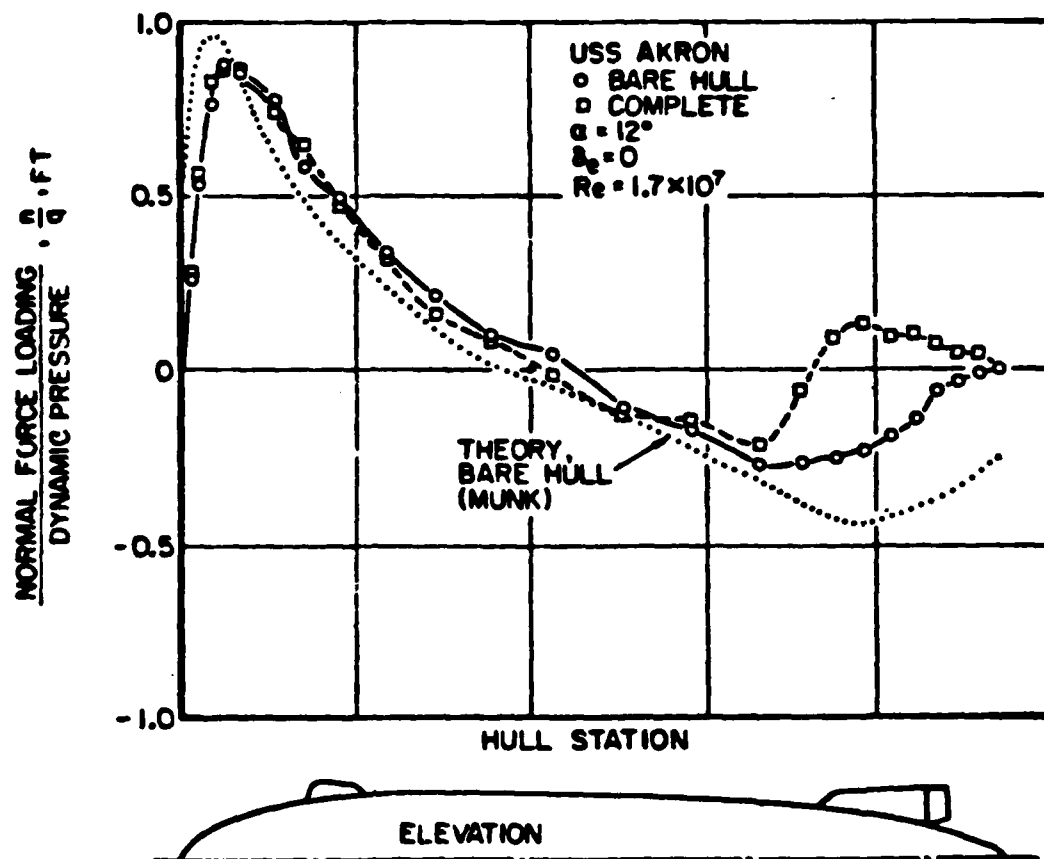


Figure 3.2 Comparison of Experimental and Theoretical Normal Force Loading on Airship Hull (Ref. 6).

We also present a comparison of the equivalent area concept with the present theory in Figure 3.1. If we calculate the integral of $g(x)$, i.e., the total load, we get

$$g_0^N = \int_{-1}^1 g(x)dx = A_0' \int_{-1}^1 F(x)dx \quad (3.27)$$

On the other hand, the integral of the slender body load up to station x_0 is

$$g_0^{N'} = - \int_{-1}^{x_0} x dx = \frac{1 - x_0^2}{2} \quad (3.28)$$

If the equivalent area is selected so that $g_0^N = g_0^{N'}$, we obtain

$$x_0 = \left[1 - 2A_0' \int_{-1}^1 F(x)dx \right]^{1/2} \quad (3.29)$$

where integrals of the eigenfunction are given in Table 3.1.

TABLE 3.1

N	$\int_{-1}^1 F(x) dx$	$\int_{-1}^1 xF(x) dx$
5	0.778	0.423
6	0.704	0.401
7	0.645	0.380
8	0.596	0.361
9	0.555	0.344
10	0.520	0.329
11	0.490	0.315

For $N = 7$ we find that

$$x_0 = 0.6 \quad (3.30)$$

Thus, if the slender body load is truncated at $x_0 = 0.6$ (point A in Figure 3.1), the total lift is the same as that obtained with the present theory for $A'_0 = 1/2$. However, the equivalent base area load distribution bears very little resemblance to measured data like those in Figure 3.2.

To conclude this section, we calculate a typical value of A'_0 from experimental data. The lift and moment coefficients versus angle of attack for the USS Akron Bare Hull and complete configuration are presented in Figure 2.3 (also from Ref. 6). The coefficients are normalized as follows:

$$\begin{aligned} \bar{C}_N &= \frac{\text{Lift}}{q_\infty (V)^{2/3}} \\ \bar{C}_M &= \frac{\text{Moment}}{q_\infty (V)^{2/3} \cdot l} \end{aligned} \quad (3.31)$$

where V is the hull volume. For the prolate spheroid

$$V = \frac{2\pi}{3} \cdot R_0^2 \cdot l \quad (3.32)$$

where R_0 is the maximum body radius. We compare Eqs. (2.11), (3.24) and (3.32) to obtain the following expression for A'_0 :

$$A'_0 = \frac{2}{\pi} \cdot \frac{d\bar{C}_N/d\alpha}{\frac{(6\epsilon/\pi)^{2/3}}{1+\epsilon} \int_{-1}^1 F(x)dx} \quad (3.33)$$

From Figure 3.3 we have

$$\frac{d\bar{C}_N}{d\alpha} = .0057/\text{deg} = .33/\text{rad} \quad (3.34)$$

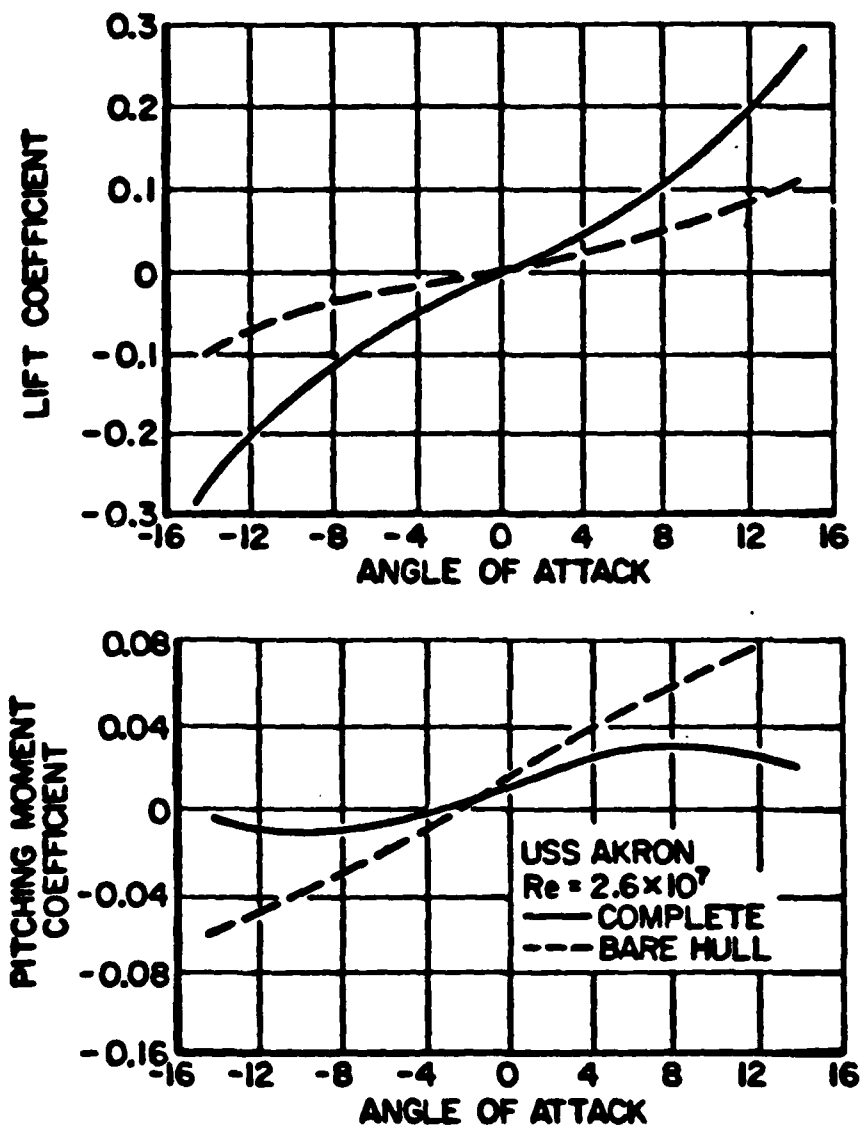


Figure 3.3 Variation of Lift and Pitching Moment Coefficients with Angle of Attack (Ref. 5).

and

$$\epsilon = 1/5.9 = .169 \quad (N \approx 6) \quad (3.35)$$

Thus

$$A'_0 = .45 \quad (3.36)$$

We conclude that the results shown in Figure 3.1 for $A'_0 = 0.5$ are typical for body fineness ratios of order 6 or 7.

The results presented in this report have focused on the proper formulation of inviscid slender body theory. In conclusion, we remark that the viscous integral equations corresponding to our fundamental result, Eq. (2.32), can be written down at once following the procedure outlined in Section II E of Ref. 1. We simply replace the Cauchy singular part of the kernel function with its viscous form to get

$$\frac{\tau(x)}{\pi} \int_{-1}^1 L(y) \frac{\partial}{\partial x} \left[\ln|x-y| + e^{\sigma(x-y)} K_0(\sigma|x-y|) \right] dy = \tau(x) \alpha(x) \quad (3.37)$$

where $K_0(z)$ is the modified Bessel function and σ is the Reynolds number based on an "appropriate" body length scale (e.g., the half length or a typical radius). The final step is the development of the viscous theory in order to solve Eq. (3.37) and calculate A'_0 as a function of Reynolds number. This step will be a breakthrough insofar as our fundamental understanding of the origin of lift on a body of revolution and in our ability to calculate lift from first principles. It is anticipated that the viscous work can be completed in a future research effort.

IV. CONCLUSIONS .

1. To calculate the inviscid lift distribution on a slender body of revolution, the essential Cauchy singularity must be retained in the integral equation that relates the load and upwash functions.
2. The asymptotic slender body theory derived herein has an exact solution for a prolate spheroidal body. The eigenfunction is a hypergeometric or incomplete Beta function.
3. The lift coefficient for a slender body is proportional to the coefficient of the eigenfunction in complete analogy with the theory of lift on wing sections.
4. The coefficient of the eigenfunction is of order unity for typical slender bodies.
5. The qualitative features of the load distribution are in much better agreement with experimental data than the distribution obtained with the equivalent base area concept applied to conventional slender body theory.
6. The theory can readily be modified to include viscosity following the procedure outlined in Section II E of Ref. 1.

V. REFERENCES

1. Yates, John E.: Viscous Theory of Lift on Bodies of Revolution. A.R.A.P. Report No. 464, Aeronautical Research Associates of Princeton, Inc., February 1982.
2. Ribner, Herbert S.: The Ring Airfoil in Nonaxial Flow. Journal of Aeronautical Sciences, Vol. 14, No. 9, pp. 529-530, September 1947.
3. Flatau, Abraham: Feasibility Study of the 2.5-Inch Ring Airfoil Grenade (RAG), (A Review and Summary). Department of the Army, Edgewood Arsenal Technical Report EATR 4573, December 1971.
4. Abramowitz, M. and Stegun, I. A., eds.: Handbook of Mathematical Functions (2nd Printing), National Bureau of Standards, Washington, DC, 1964.
5. Lamb, Horace: Hydrodynamics (6th Edition). Dover Publications, New York, 1932.
6. Curtiss, H. C., Jr., Hazen, D. C., and Putman, W. F.: LTA Aerodynamic Data Revisited. J. Aircraft, Vol. 13, No. 11, pp.835-844, November 1976.

DATE
ILME